

each other could explain the remarkable efficacy of anti-HMGB1 mAb therapy in TBI.

In other words, the action of HMGB1 could be present upstream of the secondary responses in TBI, triggering a cascade of events leading to BBB disruption, brain edema, and brain injury.<sup>1,33</sup>

Consistent with the reduction in brain edema and decrease in the resultant brain lesion observed with anti-HMGB1 mAb, this therapy significantly improved the acute motor impairments induced by percussion injury throughout the observation period, except at 3 hours after injury. Thus, protection of the BBB from disruption as well as the control of inflammatory responses by treatment with anti-HMGB1 mAb accompanied the maintenance of CNS motor function. Hematoxylin-eosin and Nissl staining of brain sections from control rats revealed a considerable loss of neurons in the cerebral cortex whereas the area of neuronal loss was restricted to the surface of the cerebral cortex in anti-HMGB1-treated rats. These histological findings were consistent with the neurological evaluation data.

Intravenously administered recombinant HMGB1 dose-dependently exacerbated the increase in BBB permeability and motor impairment in rats receiving moderate percussion injury. Therefore, it is possible that circulating endogenous HMGB1 plays an important role in the development of BBB disruption and brain inflammation, especially through the stimulation of vascular endothelial cells and blood cells. Indeed, anti-HMGB1 mAb significantly inhibited the expression of plasminogen activator inhibitor-1, a marker of vascular endothelial cell activation, and neutrophil elastase, suggesting that the interaction between vascular endothelial cells and blood cells was reduced<sup>5,34</sup> through the clearance of circulating HMGB1 by specific mAb (Fig 7D).

These aspects await clarification in future studies.

It has been reported that the effects of HMGB1 are mediated by plural receptors; i.e., receptor for advanced glycation endproducts (RAGE)<sup>12, 13</sup> and toll-like receptor-2/4 (TLR-2/4).<sup>14-16</sup> To examine the relative involvement of these receptors, we conducted studies using the respective gene knockout- and wild-type mice. From these experiments, it could be concluded that RAGE is predominantly involved in the mediation of HMGB1 effects because the increase in BBB permeability induced by percussion injury was much less in RAGE<sup>-/-</sup> mice compared with wild-type mice and the inhibitory effects of anti-HMGB1 mAb observed in wild-type mice disappeared in RAGE<sup>-/-</sup> mice. Concerning the TLR-2/4, the phenotype in knockout mice was intermediate and not so conclusive. Thus, further works in this area is needed.

Judging from the remarkable efficacy of anti-HMGB1 mAb in the therapy of rat TBI, as well its putative mechanisms, this novel therapy could be applicable for clinical use. Since uncontrolled brain edema leading to brain herniation is one of the main causes of death in patients after TBI,<sup>1</sup> early treatment with anti-HMGB1 mAb might be a promising strategy for TBI. In addition, patients with TBI often experiences posttraumatic epilepsy<sup>35, 36</sup> and impairment in cognitive function.<sup>37</sup> Moreover, TBI has been considered as a risk factor for Alzheimer's disease.<sup>38</sup> Accordingly, it is possible that anti-HMGB1 mAb therapy might inhibit the secondary brain injury arising from TBI, and thereby greatly improve the prognosis for this condition and reduce the incidence of complications.

In conclusion, anti-HMGB1 mAb efficiently reduced acute brain edema after TBI through protection of the BBB and inhibition of the inflammatory responses. It was

strongly suggested that endogenous HMGB1 may play plural and crucial roles in the early events of TBI and that the processes mediated by HMGB1 may be present upstream in the sequence of events. We propose mAb therapy as a novel treatment approach for TBI.

Accepted Article

### Acknowledgments

We thank M. Narasaki and S. Takagi for their technical assistance. This work was supported by grants from the Scientific Research from the Ministry of Health, Labor and Welfare of Japan, from the Japan Society for the Promotion of Science (JSPS No. 21390071, 21590594, 2365968703), and from Kyosai Research Foundation.

## References

1. Shlosberg, D., Benifla, M., Kaufer, D. & Friedman A. Blood-brain barrier breakdown as a therapeutic target in traumatic brain injury. *Nat Rev Neurol* 2010; 6: 393-403.
2. Lenzlinger, P.M., Morganti-Kossmann, M.C., Laurer H.L. & McIntosh, T. K. The duality of the inflammatory response to traumatic brain injury. *Mol Neurobiol* 2001; 24: 169-181.
3. Unterberg, A.W., Stover, J., Kress, B. & Kiening, K.L. Edema and brain trauma. *Neuroscience* 2004; 129: 1021-1029.
4. Pun, P.B.L., Lu, J. & Moochhala, S. Involvement of ROS in BBB dysfunction. *Free Rad Res* 2009; 43: 348-364.
5. Fabene, P.F. et al. A role for leukocyte-endothelial adhesion mechanisms in epilepsy. *Nat Med* 2008; 14: 1377-1383.
6. Narayan, R.K., Michel, M. E. , et al. Clinical trial in head injury. *J Neurotrauma* 2002; 19: 503-557.
7. Lotze, M.,T. & Tracey, K.J. High-mobility group box1 protein (HMGB1): nuclear weapon in the immune arsenal. *Nat Rev Immunol* 2005; 5: 331-342.
8. Andersson, U. & Tracey, K.J. HMGB1 is a therapeutic target for sterile inflammation and infection. *Annu Rev Immunol* 2011; 29: 139-162.

9. Wang, H. et al. HMG-1 as a late mediator of endotoxin lethality in mice. *Science* 1999; 285: 248–251.
10. Abraham, E., Arcaroli, J., Carmody, A., Wang, H. & Tracey KJ. HMG-1 as a mediator of acute lung inflammation. *J Immunol* 2000; 165: 2950–2954.
11. Schaffidi, P., Misteli, T. & Bianchi, M.E. Release of chromatin protein HMGB1 by necrotic cells triggers inflammation. *Nature* 2002; 418: 191-195.
12. Hori, O. et al. The receptor for advanced glycation endproducts (RAGE) is a cellular binding site for amphotericin. *J Biol Chem* 1995; 270: 25752-25761.
13. Muhammad, S. et al. The HMGB1 receptor RAGE mediates ischemic brain damage. *J Neurosci* 2008; 28: 12023–12031.
14. Park, J.S. et al. High mobility group box 1 protein interacts with multiple toll-like receptors. *Am J Physiol* 2002; 290: C917-C924.
15. Yu, M. et al. HMGB1 signals through toll-like receptor (TLR) 4 and TLR2. *Shock* 2006; 26 : 174-179.
16. Maroso, M. et al. Toll-like receptor-4 and high-mobility group box-1 are involved in ictogenesis and can be targeted to reduce seizures. *Nat Med* 2010; 16: 413-419.
17. Taniguchi, N. et al. High mobility group box chromosomal protein 1 plays a role in the pathogenesis of rheumatoid arthritis as a novel cytokine. *Arthritis Rheum* 2003; 48 : 971–981.
18. Matsuoka N. et al. High-mobility group box 1 is involved in the onitil events of early loss of transplanted islets in mice. *J Clin Invest* 2010; 120: 735-743.

19. Liu, K. et al. Anti-high mobility group box 1 monoclonal antibody ameliorates brain infarction induced by transient ischemia in rats. *FASEB J* 2007; 21: 3904–3916.
20. Zhang, J. et al. Anti-high mobility group box-1 monoclonal antibody protects the blood-brain barrier from ischemia-induced disruption in rats. *Stroke* 2011; 42: 1420-1428.
21. Otani, N., Nawashiro, H., Fukui, S., Nomura, N. & Shima, K. Temporal and spatial profile of phosphorylated mitogen-activated protein kinase pathways after lateral fluid percussion injury in the cortex of the rat brain. *J Neurotrauma* 2002; 19: 1587-1596.
22. Myint, K.M. et al. RAGE control of diabetic nephropathy in a mouse model. Effects of RAGE gene disruption and administration of low-molecular weight heparin. *Diabetes* 2006; 55: 2510-2522.
23. Qiu, J. et al. Early release of HMGB-1 from neurons after the onset of brain ischemia. *J Cereb Blood Flow Metab* 2008; 28: 927–938.
24. Dietrich, W.D. et al. Widespread hemodynamic depression and focal platelet accumulation after fluid percussion brain injury: a double-label autographic study in rats. *J Cer Blood Flow Met* 1996; 16: 481-489.
25. Stein, S.C., Graham, D.I., Chen, X.H. & Smith, D.H. Association between intravascular microthrombosis and cerebral ischemia in traumatic brain injury. *Neurosurgery* 2004; 54: 687-691.

26. Dietrich, W.D., Alonso, O. & Halley, M. Early microvascular and neuronal consequences of traumatic brain injury: a light and electron microscopic study in rats. *J Neurotrauma* 1994; 11: 289-302.
27. Higashida, T. et al. The role of hypoxia-inducible factor-1 $\alpha$ , aquaporin-4, and matrix metalloproteinase-9 in blood-brain barrier disruption and brain edema after traumatic brain injury. *J Neurosurg* 2011; 114: 92-101.
28. Yong, V.W. Metalloproteinases: mediators of pathology and regeneration in the CNS. *Nat Rev Neurosci* 2005; 6: 931-944.
29. Gahm, C., Holmin, S. & Mathiesen, T. Nitric oxide synthase expression after human brain contusion. *Neurosurg* 2002; 50: 1319-1326.
30. Khan, M. et al. Administration of S-nitroglutathione after traumatic brain injury protects the neurovascular unit and reduces secondary injury in a rat model of controlled cortical impact. *J Neuroinflam* 2009; 6: 32.
31. Yang, Y., Estrada, E. Y., Thompson, J. F., Liu, W. & Rosenberg, G. A. Matrix metalloproteinase mediated disruption of tight junction proteins in cerebral vessels is reversed by synthetic matrix metalloproteinase inhibitor in focal ischemia in rat. *J Cereb Blood Flow Metab* 2007; 27: 697-709.
32. Jafarian-Tehrani, M. et al. 1400W, a potent selective inducible NOS inhibitor, improves histopathological outcome following traumatic brain injury in rats. *Nitric Oxide* 2005; 12: 61-69.



33. Weiss, N., Miller, F., Cazaubon, S. & Couraud P.O. The blood-brain barrier in brain homeostasis and neurological diseases. *Biochim Biophys Acta* 2009; 1788: 842-857.
34. Chaicana, K.L., Pradilla, G, Huang, J. & Tamargo, R.J. Role of inflammation (leukocyte-endothelial cell interactions) in vasospasm after subarachnoid hemorrhage. *World Neurosurg* 2010; 73: 22-41.
35. van Vliet, E.A. et al. Blood-brain barrier leakage may lead to progression of temporal lobe epilepsy. *Brain* 2007; 130: 521-534.
36. Tomkins, O. et al. Blood-brain barrier breakdown following traumatic brain injury: a possible role in posttraumatic epilepsy. *Cardiovasc Psychi Neurol* 2011; Article ID 765923, 11 pages.
37. Silver, J.M., McAllister, T.W. & Arciniegas, D.B. Depression and cognitive complaints following mild traumatic brain injury. *Am J Psychiatry* 2009; 166: 653-661.
38. Guo, Z. et al. Head injury and risk of AD in the MIRAGE study. *Neurology* 2000; 54: 1316-1323.

**Figure legends****FIGURE 1:**

Time-dependent translocation of HMGB1 in neurons in the TBI site and the effects of anti-HMGB1 mAb. (A) After fluid percussion injury on the right temporal cortex (top panel), the rats received intravenous injection of anti-HMGB1 (1 mg/kg) or control mAb twice at 5 minutes and 6 hours thereafter and the brains were fixed at different time points. The brain sections were double immunostained with anti-HMGB1 and anti-MAP-2 antibodies, followed by AlexaFluor 555-labelled and AlexaFluor 488-labelled secondary antibodies, respectively. Scale bars; 50  $\mu\text{m}$  (yellow) and 5  $\mu\text{m}$  (white). (B) Decrease in HMGB1 levels in the TBI region. cerebral cortex from both sides (3 mm square) were collected 24 hours after injury for western blotting. The lane on the left side represents recombinant HMGB1.  $\beta$ -actin was used as the internal control. (C) Quantitative analyses were performed using NIH Image J software. Results are expressed as mean  $\pm$  SEM of 5 rats.  $**P < 0.01$  compared with contralateral side.  $##P < 0.01$  compared with control rats.

**FIGURE 2:**

Effect of anti-HMGB1 mAb on brain lesion and BBB permeability in rats with TBI induced by fluid percussion. (A) Histological examination of brain sections from TBI rats. The brains were fixed at 6 hours after injury and sections were stained with

hematoxylin-eosin (left) or cresyl violet (right). There were few intact neurons in the injured site in control rats whereas the numerous intact neurons remained in anti-HMGB1-treated rats. **(B)** The permeability of brain capillary vessels was examined by intravenously injecting Evans blue (40 mg/kg) at 6 hours after injury and then measuring the leakage of Evans blue-albumin into the brain parenchyma at 3 hours post-injury. **(C)** Results are expressed as the mean  $\pm$  SEM of 7 rats. \* $P < 0.05$  compared with the control group. **(D)** Albumin extravasation 6 hours after injury detected by anti-rat albumin Ab.

**FIGURE 3:**

Effect of anti-HMGB1 mAb on T2-weighted MRI. **(A)** Three representative MRIs from each group (n=5) are shown. **(B)** The quantitative evaluation was performed. Results are expressed as mean  $\pm$  SEM. of 5 rats. \*\* $P < 0.01$  compared with the control group.

**FIGURE 4:**

Effects of anti-HMGB1 mAb on the impairment of motor functions. **(A)** The results of rotarod test were expressed as mean  $\pm$  SEM of 6 rats. \* $P < 0.05$  and \*\* $P < 0.01$  compared with the sham control at each time point. # $P < 0.05$  compared with the corresponding control at the same time point. **(B)** The results of limb-use asymmetry

cylinder test were expressed as mean  $\pm$  SEM of 6 rats. \*P < 0.05 compared with the pretreatment value. #P < 0.05 compared with the control.

**FIGURE 5:**

Transmission electron microscopic observation of capillary vessels and determination of MMP activity by zymography. (A) Rat brains were fixed at 6 hour after percussion injury by transcardial perfusion with 4% paraformaldehyde and 2.5% glutaraldehyde in 0.1 M cacodylic acid buffer (pH 7.3) under deep pentobarbital anesthesia. Ultrathin sections of cerebral cortex at 3 mm anterior to the injury site were prepared. Representative images from both groups are shown. Swelling of astrocyte endfeet was indicated by asterisks. The inset shows the deformed vascular endothelial cell. (B) Swelling of astrocyte endfeet was evaluated as described previously (19). Results are expressed as mean  $\pm$  SEM of 12 samples from 4 rats. \*P < 0.05 compared with the control. (C) Zymographic determination of MMP-9 and MMP-2 activity in rats with TBI induced by fluid percussion. Brain samples were prepared by homogenization of the hemisphere (lesion site) with PBS containing proteinase inhibitor cocktail and 20  $\mu$ g protein was loaded on SDS-PAGE gels containing 1 mg/ml gelatin without heating and reducing reagents. The reaction was developed for 36 hours at 37 °C and the gel was stained with Coomassie brilliant blue. (D) The results of zymography were quantified by NIH Image J and are expressed as mean  $\pm$  SEM of 4 rats. \*P < 0.05 compared with the control.

**FIGURE 6:**

Expression of inflammation-related molecules in rats with TBI. Real-time quantitative PCR was performed for the determination of inflammation-related molecule expression. The results were normalized to the expression of GAPDH. Results are expressed as mean  $\pm$  SEM of 6 rats. \*P < 0.05, \*\*P < 0.01 compared with contralateral side. #P < 0.05, ##P < 0.01 compared with control rats.

**FIGURE 7:**

Effects of exogenous HMGB1 in rats with TBI. (A) Exacerbation of brain lesions by intravenous injection of recombinant HMGB1. Rats received moderate intensity of TBI (2.0-2.2 atm injury). Recombinant HMGB1 (19) (0.04, 0.2 and 0.4 mg/kg) were administered intravenously to rats 10 min after percussion injury. BBB permeability was determined by Evans blue leakage during a 3-hour period beginning 6 hours after the induction of TBI as described in Figure 2B. (B) Results are expressed as mean  $\pm$  SEM of 5 rats. \*P < 0.05 compared with the albumin control. (C) The rotarod test was performed and the results are expressed as mean  $\pm$  SEM of 5 rats. \*P < 0.05 compared with the albumin control. (D) Determination of plasma levels of HMGB1 by ELISA in rats with TBI. Blood samples were collected 6 hours after induction of injury. Results are expressed as mean  $\pm$  SEM of 6 rats. \*P < 0.05 compared with

non-injured rats (Sham). <sup>#</sup>P < 0.05 compared with control IgG-treated rats.

**FIGURE 8:**

TBI in mice deficient in RAGE, TLR-4 or TLR-2. (A) TBI was induced in RAGE<sup>-/-</sup>, TLR-4<sup>-/-</sup>, and TLR-2<sup>-/-</sup> mice and their wild-type as described for the TBI model. Anti-HMGB1 mAb or control IgG was injected 5 minutes postinjury. BBB permeability was assessed by measurement of Evans blue leakage. Results are expressed as mean ± s.e.m. of 5 mice. <sup>\*\*</sup>P < 0.01 compared with control IgG-treated group. <sup>##</sup>P < 0.01 compared with wild-type (WT) mice. (B) Coordinated motor function was evaluated using the rotarod test as shown in Figure 2d. Results are expressed as mean ± s.e.m. of 5 mice. <sup>\*</sup>P < 0.05 compared with the respective sham control. <sup>##</sup>P < 0.01 compared with the respective control. <sup>\$</sup>P < 0.05 compared with wild-type (WT) mice.

Table1 Percussion injury and physiological parameters in rats

Percussion (atm)	Control IgG (n=10)		αHMGB1 (n=10)	
	2.38 ±0.03		2.41 ±0.02	
	Pre (n=5)	Control IgG (n=4)	αHMGB1 (n=4)	
Glucose	117 ±29	277 ±29	223 ±10	
Na	137.8 ±1.5	129.0 ±1.7	127.0 ±3.1	
K	3.06 ±0.34	3.93 ±0.08	3.88 ±0.15	
tCO <sub>2</sub>	24.2 ±2.7	33.3 ±1.0	32.8 ±1.0	
iCa	0.99 ±0.15	1.16 ±0.05	1.06 ±0.08	
Hct	36.8 ±5.0	38.8 ±2.3	38.3 ±2.6	
Hb	12.5 ±1.7	13.2 ±0.8	13.0 ±0.9	
pH	7.32 ±0.04	7.47 ±0.02	7.47 ±0.02	
pCO <sub>2</sub>	44.3 ±4.2	43.3 ±0.7	42.6 ±2.4	
pO <sub>2</sub>	283 ±60	276 ±13	221 ±51	
HCO <sub>3</sub>	22.8 ±2.7	31.8 ±0.9	31.2 ±1.0	
BE	-3.0 ±3.0	8.0 ±1.1	7.5 ±1.0	
sO <sub>2</sub>	99.4 ±0.6	100 ±0	99 ±1	

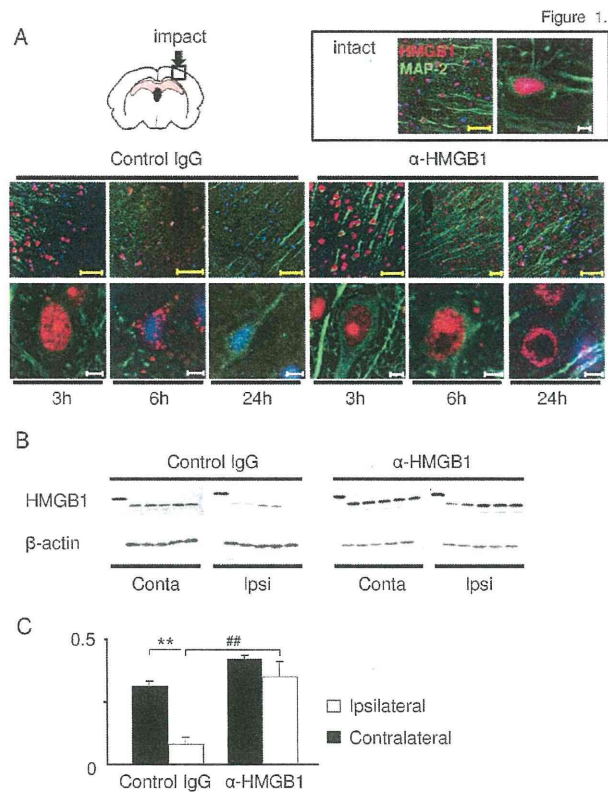
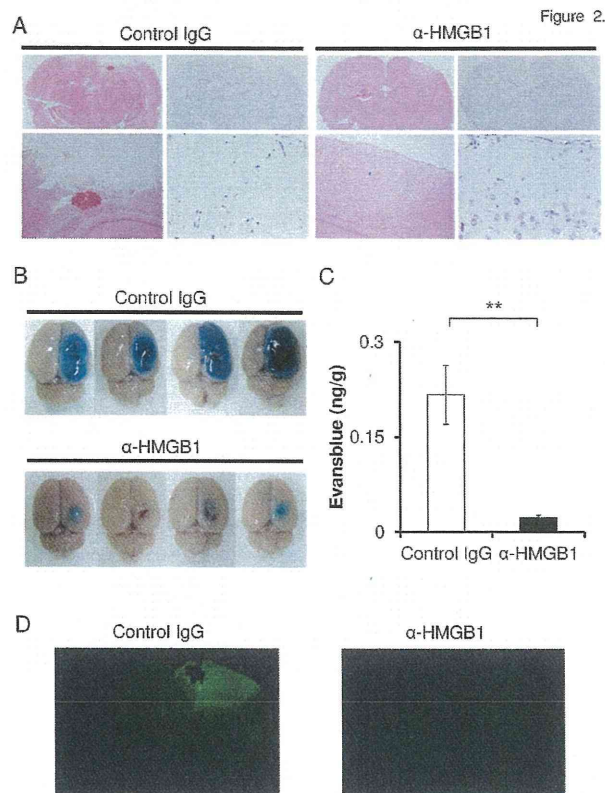


FIGURE 1:

Time-dependent translocation of HMGB1 in neurons in the TBI site and the effects of anti-HMGB1 mAb. (A) After fluid percussion injury on the right temporal cortex (top panel), the rats received intravenous injection of anti-HMGB1 (1 mg/kg) or control mAb twice at 5 minutes and 6 hours thereafter and the brains were fixed at different time points. The brain sections were double immunostained with anti-HMGB1 and anti-MAP-2 antibodies, followed by AlexaFluor 555-labelled and AlexaFluor 488-labelled secondary antibodies, respectively. Scale bars; 50  $\mu$ m (yellow) and 5  $\mu$ m (white). (B) Decrease in HMGB1 levels in the TBI region, cerebral cortex from both sides (3 mm square) were collected 24 hours after injury for western blotting. The lane on the left side represents recombinant HMGB1.  $\beta$ -actin was used as the internal control. (C) Quantitative analyses were performed using NIH Image J software. Results are expressed as mean  $\pm$  SEM of 5 rats. \*\* $P < 0.01$  compared with contralateral side. ## $P < 0.01$  compared with control rats.





**FIGURE 2:**

Effect of anti-HMGB1 mAb on brain lesion and BBB permeability in rats with TBI induced by fluid percussion. (A) Histological examination of brain sections from TBI rats. The brains were fixed at 6 hours after injury and sections were stained with hematoxylin-eosin (left) or cresyl violet (right). There were few intact neurons in the injured site in control rats whereas the numerous intact neurons remained in anti-HMGB1-treated rats. (B) The permeability of brain capillary vessels was examined by intravenously injecting Evans blue (40 mg/kg) at 6 hours after injury and then measuring the leakage of Evans blue-albumin into the brain parenchyma at 3 hours post-injury. (C) Results are expressed as the mean  $\pm$  SEM of 7 rats. \* $P < 0.05$  compared with the control group. (D) Albumin extravasation 6 hours after injury detected by anti-rat albumin Ab.

209x297mm (300 x 300 DPI)

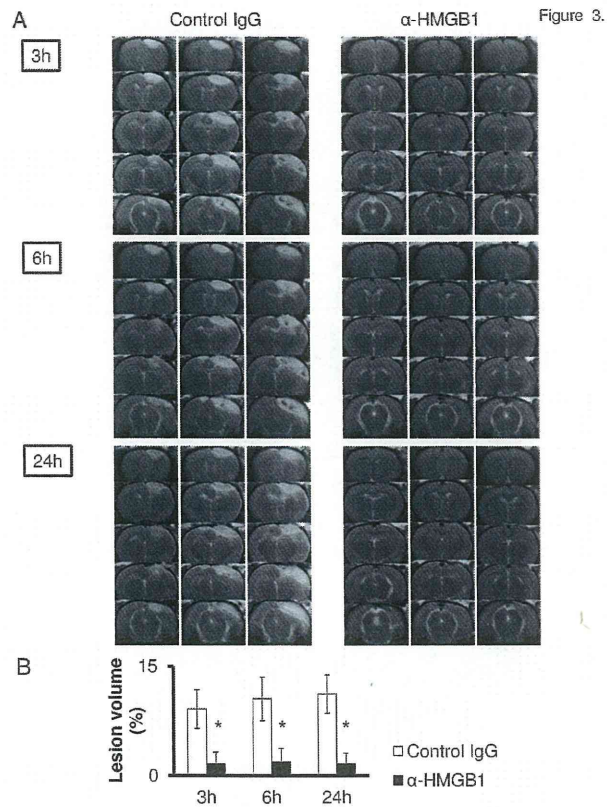


**FIGURE 3:**  
Effect of anti-HMGB1 mAb on T2-weighted MRI. (A) Three representative MRIs from each group (n=5) are shown. (B) The quantitative evaluation was performed. Results are expressed as mean  $\pm$  SEM, of 5 rats. \*\*P < 0.01 compared with the control group.

209x297mm (300 x 300 DPI)

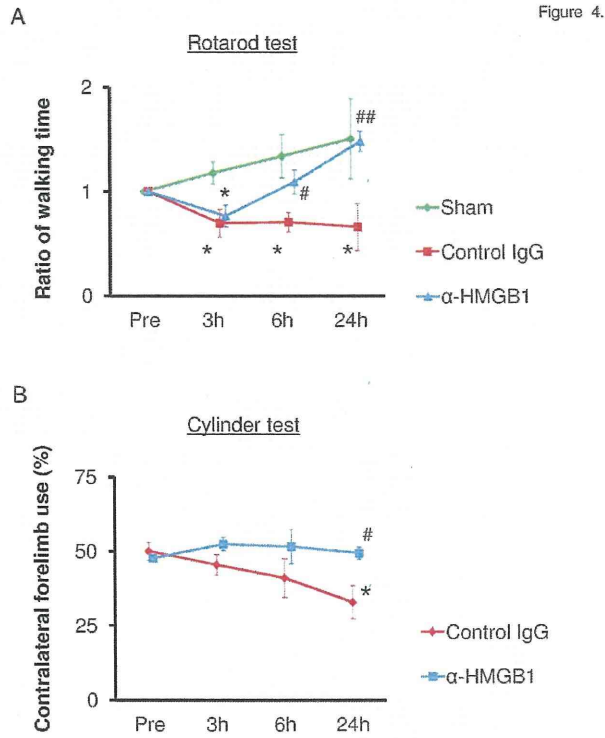


**FIGURE 4:**

Effects of anti-HMGB1 mAb on the impairment of motor functions. (A) The results of rotarod test were expressed as mean  $\pm$  SEM of 6 rats. \* $P < 0.05$  and \*\* $P < 0.01$  compared with the sham control at each time point. # $P < 0.05$  compared with the corresponding control at the same time point. (B) The results of limb-use asymmetry cylinder test were expressed as mean  $\pm$  SEM of 6 rats. \* $P < 0.05$  compared with the pretreatment value. # $P < 0.05$  compared with the control.

209x297mm (300 x 300 DPI)

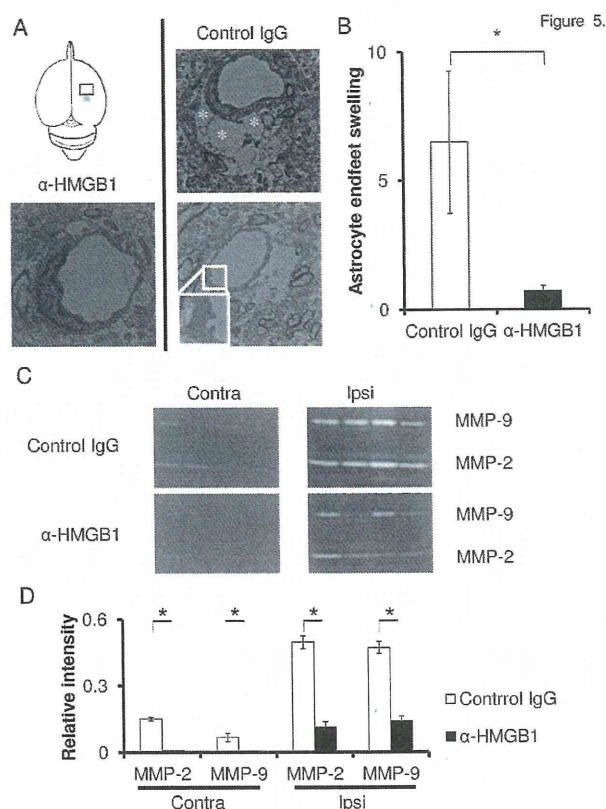


FIGURE 5:

Transmission electron microscopic observation of capillary vessels and determination of MMP activity by zymography. (A) Rat brains were fixed at 6 hours after percussion injury by transcardial perfusion with 4% paraformaldehyde and 2.5% glutaraldehyde in 0.1 M cacodylic acid buffer (pH 7.3) under deep pentobarbital anesthesia. Ultrathin sections of cerebral cortex at 3 mm anterior to the injury site were prepared. Representative images from both groups are shown. Swelling of astrocyte endfeet was indicated by asterisks. The inset shows the deformed vascularendothelial cell. (B) Swelling of astrocyte endfeet was evaluated as described previously (19). Results are expressed as mean  $\pm$  SEM of 12 samples from 4 rats. \* $P < 0.05$  compared with the control. (C) Zymographic determination of MMP-9 and MMP-2 activity in rats with TBI induced by fluid percussion. Brain samples were prepared by homogenization of the hemisphere (lesion site) with PBS containing proteinase inhibitor cocktail and 20 mg protein was loaded on SDS-PAGE gels containing 1 mg/ml gelatin without heating and reducing reagents. The reaction was developed for 36 hours at 37 °C and the gel was stained with Coomassie brilliant blue. (D) The results of